2005

Accounting for Nonlinearities in Mathematical Modelling of Quantum Dot Molecules

Roderick V.N. Melnik
Wilfrid Laurier University, rmelnik@wlu.ca

Benny Lassen
Syddansk University

L.C. Lew Yan Voon
Wright State University

Morten Willatzen
Syddansk University

Calin Galeriu
Worcester Polytechnic Institute

DISCRETE AND CONTINUOUS
DYNAMICAL SYSTEMS
Supplement Volume 2005

Website: http://AIMsciences.org

pp. **642–651**

ACCOUNTING FOR NONLINEARITIES IN MATHEMATICAL MODELLING OF QUANTUM DOT MOLECULES

R.V.N. Melnik[1], B. Lassen[2], L. C Lew Yan Voon[3],
M. Willatzen[2], C. Galeriu[4]

[1]Mathematical Modelling and Computational Sciences,
Wilfrid Laurier University, 75 University Ave W.,
Waterloo, ON, N2L 3C5, Canada

[2]Mads Clausen Institute, Syddansk University
Grundtvigs Alle 150, DK-6400 Sonderborg, Denmark

[3]Department of Physics, Wright State University,
3640 Colonel Glenn Highway, Dayton,
OH 45305, United States

[4]Department of Physics, Worcester Polytechnic Institute,
100 Institute Road, Worcester, MA 01609, United States

Abstract.

Nonlinear mathematical models are becoming increasingly important for new applications of low-dimensional semiconductor structures. Examples of such structures include quasi-zero-dimensional quantum dots that have potential applications ranging from quantum computing to nano-biological devices. In this contribution, we analyze presently dominating linear models for bandstructure calculations and demonstrate why nonlinear models are required for characterizing adequately optoelectronic properties of self-assembled quantum dots.

1. **Introduction.** The process of the formation of quantum dots (QD), and more generally, low-dimensional semiconductor nanostructures (LDSN), is complex and, in its essence, it is a competition between the surface energy in the structure and strain energy. Most of the currently used technologies are based on self-assembly where we obtain many self-assembled dots sitting on the wetting layer and distributed over it in a highly non-uniform manner. They have different size, shape, and properties. Nonlinear effects may become important in such structures, but most mathematical models discussed in the literature up to date are linear models. This applies also to the models for strain effects in such structures. Strain effects may substantially influence overall nanostructure properties and their accurate calculation is becoming increasingly important for current and potential applications of LDSNs (e.g., [5]).

Mathematical models for semiconductors to study electronic properties of single charge carriers in the context of optical properties of semiconductor quantum structures have achieved a high degree of maturity. Nevertheless, new applications of LDSN (e.g., [6, 13, 14] and references therein) led to a situation where the

2000 *Mathematics Subject Classification.* Primary: 35, 65, 81.
Key words and phrases. quantum dots, modeling, coupled PDEs, strain, bandstructures.

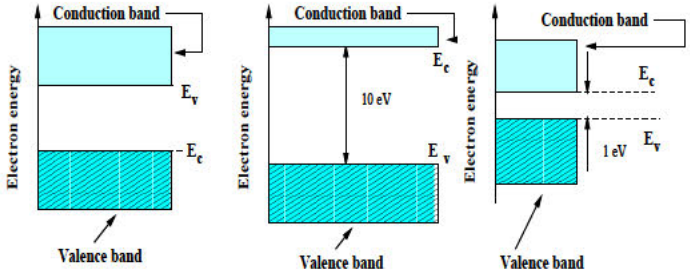

FIGURE 1. Electric properties of solids: (a) conductors, (b) insulators, (c) semiconductors.

backbone of such models - the linear Schrodinger model in the steady-state approximation - may become inadequate. Furthermore, experimental results (e.g., [15]) indicate that new effects such as strain relaxation may influence substantially on optoelectromechanical properties of the nanostructures.

In this paper, we review a hierarchy of mathematical models for studying electronic properties of low-dimensional semiconductor nanostructures. We propose several generalizations of such models in the context of strain effects for hexagonal WZ GaN/AlN quantum dots and arrays that can account for geometric and material nonlinearities. We also discuss piezoelectric effects in these models. Finally, we give details of variational formulations of the models and provide several representative examples of computational experiments.

2. **Brief Physical Overview.** Recall that bonding of atoms to form molecules of matter occurs through the interaction of the valence electrons of each atom. Electrons have a dual nature and the values of electron energies are represented by energy level diagrams. In solids atoms are brought together in such a way that the energy levels of individual atoms form bonds of energies. Electrical properties of matter are determined by 3 main energy bands, namely (a) valence band, (b) conduction band, and (c) forbidden band (or gap). In order to move into the conduction band, the valence electrons must bridge an energy gap, which determines whether a solid acts as a conductor, a semiconductor, or an insulator. Unlike in insulators, in semiconductors enough energy is provided to the valence electrons to enable them to cross the energy gap and exist as conduction (free) electrons in the conduction band (see Fig. 1). Broadly speaking, there are 2 types of semiconductors, intrinsic and doped semiconductors. In an intrinsic (pure) solid, the number of electrons in the conduction band equals to the number of holes (electron vacancies) in the valence band. Electrons and holes always generate and recombinate in pairs and, as a result, in the general case we have to talk about electron-hole pairs that in their dynamic motion form electron-hole plasma (EHP). We also differentiate between n-type and p-type semiconductors. The energy level at which a state has a probability of occupancy of 0.5 (the Fermi level) in n-type semiconductors lies toward the top end of the band gap, while in p-type semiconductors it lies toward its bottom end (see Fig. 2).

3. **Hierarchy of Mathematical Models for EHP.** The basis of mathematical modelling of semiconductors is provided by the Liouville equation for the evolution

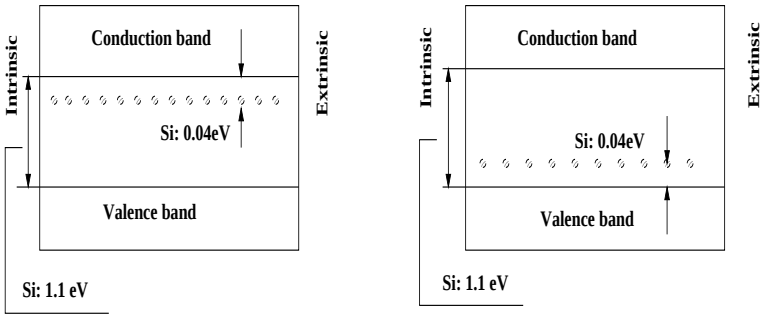

FIGURE 2. Doped semiconductors: (a) n-type, (b) p-type.

of the position-velocity probability density $f(x, v, t)$ (e.g., [7]):

$$\frac{\partial f}{\partial t} + v \cdot \mathrm{grad}_x f + 1/m\mathcal{F} \cdot \mathrm{grad}_v f = 0, \tag{1}$$

$$t > 0,\ x \in \mathbb{R}^{3M},\ v \in \mathbb{R}^{3M},$$

$$f(x, v, t = 0) \geq 0,\ \int\int f(x, v, t = 0)dxdv = 1,$$

$$\mathcal{F} = -qE \ \text{ or } \ \mathcal{F} = -q(E + v \times B_{ind}).$$

There are two limiting situations of this model that play a special role. An idealized collisionless situation is modelled with the Vlasov equation

$$\partial_t F + v \cdot \mathrm{grad}_x F + 1/m\mathcal{F}_{eff} \cdot \mathrm{grad}_v F = 0,$$
$$t > 0,\ x \in \mathbb{R}^3,\ v \in \mathbb{R}^3, \tag{2}$$

where the function $F(x, v, t)$ is the existence probability of a particle at the state (x, v) at time t and

$$E_{eff}(x, t) = E_{ext}(x, t) +$$
$$\int n(\tilde{x}, t)E_{int}(x, \tilde{x})d\tilde{x},\ \mathcal{F} = -qE_{eff},$$

or $\mathcal{F} = -q(E_{eff} + v \times B_{eff})$ (supplemented by the Maxwell system). The nature of nonlinearity in this model is defined only by the effective field equation. In particular, note that for the Coulomb force

$$E_{int} = -\frac{q}{4\pi\epsilon_s}\frac{x - y}{|x - y|^3}$$

under the assumption $E_{eff} = -\mathrm{grad}_x V_{eff}$ the effective field equation is reducible to the Poisson equation

$$-\epsilon_s \triangle V_{eff} = \rho.$$

In this case, the integration of the Vlasov equation leads to a macroscopic conservation law:

$$q\partial_t n - \mathrm{div} J = 0,$$

where $J = -q\int vFdv$ is the current density. However, in general this model is not appropriate in large-time scale modelling.

For sufficiently large time scales, the motion of particles depends decisively on scattering that is on the short-range forces:

$$\partial_t F + v \cdot \mathrm{grad}_x F + 1/m\mathcal{F}_{eff} \cdot \mathrm{grad}_v F = Q(F). \tag{3}$$

where $F(x,v,t)$ is the number density. In this case, nonlinearity is defined by the effective field model and by the model for collisions. Mathematically speaking, the situation where $\triangle v \to \infty \ \wedge \ \triangle x \to 0$ is not excluded, but in applications this situation is prohibited by allowing for non-zero relaxation time which requires that the Pauli principle be satisfied.

The Collision operator in (3) can be introduced as in [7]

$$Q(F) = \int \big\{ s(x,v',v)F(x,v',t)[1-F(x,v,t)] - s(x,v,v')F(x,v,t)[1-F(x,v't)] \big\} dv',$$

where s is the scattering (or transition) rate which is highly non-regular function. The average time between two consecutive collisions at (x,k) (the relaxation time) can be introduced as follows

$$\tau(x,k) = 1/\lambda(x,k), \ k \in B,$$

where the collision frequency is defined as

$$\lambda = \int s(x,k,k')dk'$$

with integral taken over the Brillouin zone B of the lattice.

Hydrodynamic models for semiconductors provide a computationally efficient approximations to (3). In particular, if magnetic field is ignored the hydrodynamic (more precisely, electro-hydrodynamic) model has the following form:

$$\begin{cases} \partial_t n + \partial_x(nv) = (\partial_t n)_{col}, \\ \partial_t p + \partial_x(pv + nT) = -qnE + (\partial_t p)_{col}, \\ \partial_t W + \partial_x(vW + vnT) = -qnvE - \partial_x n\tilde{Q} + (\partial_t W)_{col}, \end{cases} \tag{4}$$

where it is assumed

$$p = mnv, \ \ W = 3nT/2 + mnv^2/2,$$

$$\tilde{Q} = -\partial_x(kT).$$

The system is supplemented by the field equation, for example, by the Poisson equation:

$$\partial_{xx}(\epsilon_0 \epsilon\varphi) = -q(N_D - N_A - n).$$

Note that the hierarchy of the models for semiconductors can be classified based on relaxation times. Observe first that in the general case, due to the presence of collision terms the type of the differential equations changes with respect to the functional dependency between $(\partial_t n)_{col}$, $(\partial_t p)_{col}$, and $(\partial_t W)_{col}$ and the form of this dependency can be established only through experiments. Since in applications it is reasonable to approximate the collision terms by relaxation time approximations, the hierarchy of the mathematical models with respect to the dependencies between τ, τ_ω (relaxation of energy) and τ_p (relaxation of momentum) is the most natural.

In many practically important cases, we use the following (quasi-)hydrodynamic model [8]:

$$\begin{cases} \partial_{xx}\varphi = q(n - p - N)/\epsilon\epsilon_0 \\ \partial_t n - \partial_t J_n/q = F, \\ \partial_t p + \partial_t J_p/q = F, \\ \partial_t \bar{\mathcal{E}}_n + \partial_x Q_n = -J_n \partial_x \varphi + P_n, \\ \partial_t \bar{\mathcal{E}}_p + \partial_x Q_p = J_p \partial_x \varphi + P_p, \end{cases} \tag{5}$$

where expressions for densities of carrier currents, J_n, J_p and flux energies, Q_n and Q_p have the following form

$$J_n = -qn\mu_n\partial_x\varphi + \partial_x(T_n\mu_n n), \quad J_p = -qp\mu_p\partial_x\varphi - \partial_x(T_p\mu_p p),$$

$$Q_n = \beta_n T_n n\mu_n\partial_x\varphi - \beta_n\partial_x[T_n D_n n]/q,$$

$$Q_p = -\beta_p T_p p\mu_p\partial_x\varphi - \beta_p\partial_x[T_p D_p p]/q.$$

Now, we are in a position to introduce also quantum effects into the model. Indeed, the smooth quantum hydrodynamic approximation has the same form as above, but constitutive relations for the stress tensor, energy density, and the heat flux incorporate both classical and quantum effects. Compared to the classical Schrodinger's model, this approach offers a substantial computational speed-up. Note that the above hierarchy of the models has been constructed based on a transformation of continuum (fluid dynamics like) models into a new model in order to account for discretness of the problem. At the same time, we can approach the problem in a different way, moving from discrete models to continuum-based models. Such a fundamental approach to modelling quantum semiconductor devices is based on the mixed-state Schrodinger equation coupled to Poisson's equation for the electrostatic potential. The complexity of the problem becomes clear if we notice that, in its generality, the problem has to be considered in 6 dimensions (for position and momentum).

4. **Models for bandstructure calculations of LDSN.** Full energy spectrum of even a single symmetric quantum dot, including Coulomb interactions between charges and other effects, is a very complex task in itself. Moreover, self-assembled semiconductor QD nanostructure is an array (or a molecule) of many individual quantum dots sitting on the same "substrate" (the wetting layer). As AFM images reveal, the distribution of such quantum dots on this substrate is highly non-uniform. Each such a dot contains several hundred thousand atoms. If we attempt to apply to this problem ab initio or atomistic methodologies in order to account for quantum effects, we will get a task of enormous computational complexity in solving such a large-scale many-body problem. Surely, taken each quantum dot in isolation, the task can be managed as computational runs with over 20 million atom simulations have been reported in the literature (e.g., [12]. However, accounting for the wetting layer (even in the individual quantum dot model [9] would increase the computational complexity of the problem in several times. Even if we would do such large scale atomic simulations, in calculating atomic positions the definitions of atomic forces that enter the Hamiltonian in such large scale atomic simulations are approximate. In addition, in a number of cases we have to be able to incorporate into the model other effects such as piezoelectric.

What is needed in this situation is to apply an averaging procedure over atomic scales. Such procedures are available, including those based on empirical tight-binding, pseudopotential, and $k \cdot p$ approximations. The $k \cdot p$ approximation represents the electronic structure in a continuum-like manner and is well suited for incorporating additional effects into the model such as strain and piezoelectric effects.

In what follows we focus on WZ materials. These materials are hexagonal and the resulting problem is mathematically more challenging compared to ZB materials. From an application point of view, strain and piezoelectric effects are substantially more pronounced in such structures as compared to cubic materials.

Next we note that the accuracy of the $k \cdot p$ (the envelope function) approximation depends on the choice of the functional space where the envelope function is considered. Hence, our next step would be to explain the choice of subbands for our WZ materials models. The basis functions that span such a space correspond to subbands within conduction and valence bands of the semiconductor material. The number of basis functions that is typically chosen in approximations ranges from 1 to 8. This choice is a balance between the accuracy of the model and computational feasibility of its solution. Physical effects for the WZ materials that are desirable to include into the model are spin-orbit and crystal-field splitting, as well as valence and conduction band mixing (due to a large band gap typical for these materials). Hence, we use 6 valence subbands and 2 conduction subbands (accounting for spin up and down situations) and will be solving the following PDE eigenvalue problem with respect to eigenpair (Ψ, E):

$$H\Psi = E\Psi, \quad \Psi = (\psi_S^{\uparrow}, \psi_X^{\uparrow}, \psi_Y^{\uparrow}, \psi_Z^{\uparrow}, \psi_S^{\downarrow}, \psi_X^{\downarrow}, \psi_Y^{\downarrow}, \psi_Z^{\downarrow})^T \tag{6}$$

where

- $\psi_X^{\uparrow} \equiv (|X> \mid \uparrow)$ denotes the wave function component that corresponds to the X Bloch function of the valence band with the spin function of the missing electron "up",
- the subindex "S" denotes the wave function component of the conduction band, etc,
- E is the electron/hole energy.

The Hamiltonian in (6) is taken in the form of $k \cdot p$ theory

$$H \equiv H^{(\alpha,\beta)}(\vec{r}) = -\frac{\hbar^2}{2m_0} \nabla_i \mathcal{H}_{ij}^{(\alpha,\beta)}(\vec{r}) \nabla_j, \tag{7}$$

where $\mathcal{H}$ is the energy functional defined either by the standard Kohn-Luttinger Hamiltonian, or as its Burt-Foreman correction. It represents the kinetic energy plus a nonuniform potential field and other effects contributing to the total potential energy of the system. The superindeces (α, β) denote a basis for the wave function of the charge carrier, so that in our case we have an 8×8 matrix Hamiltonian.

5. **Strain effects in LDSN and associated nonlinearities.** Accounting for strain effects in this model provides a link between a microscopic (quasi-atomistic) description of the system with the effects that are pronounced at a larger-than-atomistic scale level as a result of interacting atoms. Atomic displacements *collectively* induce strain in our finite structure and this happens at the stage of growing the quantum dot from the crystal substrate wetting layer. This fact leads to a modification of the bandstructures obtainable for idealized situations without accounting for strain effects.

Early developments by Pikus & Bir and Rashba & Sheka led to what is now known as the Rashba-Sheka-Pikus (RSP) Hamiltonian. This Hamiltonian is applied here in the context of WZ materials in a way similar to [11, 3]. The question remains, however, on how to resolve adequately physical effects at edges, corners, and interfaces, including strain nonhomogeneities. We emphasize that all current models for bandstructure calculations we are aware of are based, in one way or another, on the original representation of [2] where strain is treated on the basis of infinitesimal theory with Cauchy relationships between strain and displacements. Geometric irregularities make this approximation inadequate. Since the LDSN is

initially stressed, the finite strain representation can be given by Eulerian components of the strain if we use the second order approximation:

$$\epsilon_{ij} = \frac{1}{2}\left(\partial u_i/\partial x_j + \partial u_j/\partial x_i + \frac{\partial u_k}{\partial x_i}\frac{\partial u_k}{\partial x_j}\right). \tag{8}$$

Material nonlinearities (stress-strain relationships) may also influence on the nanosystem properties. However, since strain remains of orders of magnitudes smaller of the elastic limits we use in this paper the linear relationship. In particular, for hexagonal WZ materials these relationships have the form:

$$\begin{aligned}
&\sigma_{xx} = c_{11}\epsilon_{xx} + c_{12}\epsilon_{yy} + c_{13}\epsilon_{zz} - e_{13}E_z,\\
&\sigma_{yy} = c_{12}\epsilon_{xx} + c_{11}\epsilon_{yy} + c_{13}\epsilon_{zz} - e_{31}E_z,\\
&\sigma_{zz} = c_{13}(\epsilon_{xx} + \epsilon_{yy}) + c_{33}\epsilon_{zz} - e_{33}E_z,\\
&\sigma_{yz} = c_{44}\epsilon_{yz} - e_{15}E_y,\ \sigma_{zx} = c_{44}\epsilon_{zx} - e_{15}E_x,\ \sigma_{xy} = \frac{1}{2}(c_{11} - c_{12})\epsilon_{xy},
\end{aligned} \tag{9}$$

where the coordinate subindeces (Timoshenko-Karman notations) are $1 \to x, 2 \to y, z \to 3$. These relationships couple together steady-state equations of motion:

$$\frac{\partial \sigma_{ij}}{\partial x_j} + \rho F_i(\xi_l) = 0 \tag{10}$$

and the Maxwell equation for the piezoelectric potential (assuming the external charge distribution, including ionic and free charges, negligible)

$$\nabla \cdot \mathbf{D}(r) = 0. \tag{11}$$

Here, $\mathbf{D}$ is the vector of electric displacement and other notations are standard (e.g., [10]). Finally, constitutive relationships for $\mathbf{D}$ are:

$$\begin{aligned}
&D_x = e_{15}\epsilon_{zx} + \varepsilon_{11}E_x, \quad D_y = e_{15}\epsilon_{yz} + \varepsilon_{11}E_y,\\
&D_z = e_{31}(\epsilon_{xx} + \epsilon_{yy}) + e_{33}\epsilon_{zz} + \varepsilon_{33}E_z + P_{sp},
\end{aligned} \tag{12}$$

where P_{sp} is the spontaneous polarization, and $\mathbf{E} = -\nabla\varphi$. In all computational experiments, the LDSN was embedded in a larger matrix material where Dirichlet boundary conditions for displacements are assumed.

The above problem is reformulated variationally and solved as a fully coupled problem. Known results obtained so far in the context of bandstructure calculations are based on the minimization of elastic energy only (e.g., [1, 3]), rather than on the solution of a coupled problem. Even in the linear approximation, the coupling between the field of deformation and the piezoelectric field is of fundamental importance. Indeed, neglecting coupling in strain calculations could lead to as high as a 30% error (e.g., [4]).

The above model is coupled with Schrodinger's model by noting that the weak form of the Schrodinger equation is equivalent to finding stationarity conditions for the following functional (e.g., [5]):

$$\Phi(\Psi) = -\frac{\hbar^2}{2m_0}\int_{\tilde{V}} (\nabla\Psi)^T \mathcal{H}^{(\alpha,\beta)} \nabla\Psi dv - E\int_{\tilde{V}} \Psi^T\Psi dv \tag{13}$$

with respect to the wave function vector field Ψ defined in (6). Our final comment goes to the Hamiltonian approximation, in particular valence subbands. The Hamiltonian is represented as a sum of constant and k-dependent energies:

$$H = H_0 + \tilde{\mathcal{H}}, \quad \tilde{\mathcal{H}} = H_1 + H_2 + H_3, \tag{14}$$

where H_0 (which is usually derived from the standard Kane Hamiltonian at $k = 0$) accounts for the spin-splitting effects. For the corresponding spin-orbit coupling matrix for the WZ materials we followed the ideas of [11, 3] and by noting also that the associated (with $k = 0$) matrix elements for the conduction band in (14) are zero. The second term, $\tilde{\mathcal{H}}$, consists of contributions of

- the kinetic part of the microscopic Hamiltonian unit cell averaged by the respective Bloch function (S, X, Y, or Z), denoted as H_1;
- the strain-dependent part of the Hamiltonian, denoted as H_2, and
- the energy of unstrained conduction/valence band edges, denoted as H_3.

Conduction subbands were approximated in the standard manner.

6. **Computational experiments.** Our first group of experiments was related to the modelling of a single truncated conical quantum dot. As expected, all of the six calculated states are clearly localized within the dot topology. Two representative plots are given in Figs. 3 and 4.

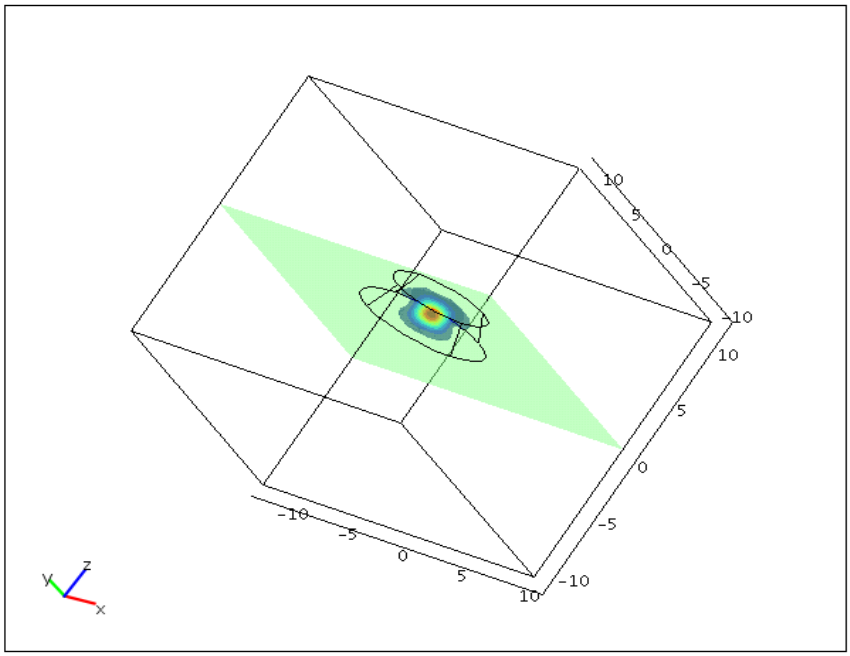

FIGURE 3. Quantum dot eigenstate that corresponds to the first eigenvalue

The situation becomes more complicated in the case of interacting quantum dots. In Fig. 5 we present the x component of displacement. As per eigenstates in this quantum dot molecule, we observe a subsequent localization of eigenstates in different dots of the structure. As optical properties of dense quantum dot arrays differ substantially from those of low-density structures and isolated idealized quantum dots, these models should contribute further to studying the effects of strain on bandstructures in such low dimensional semiconductors.

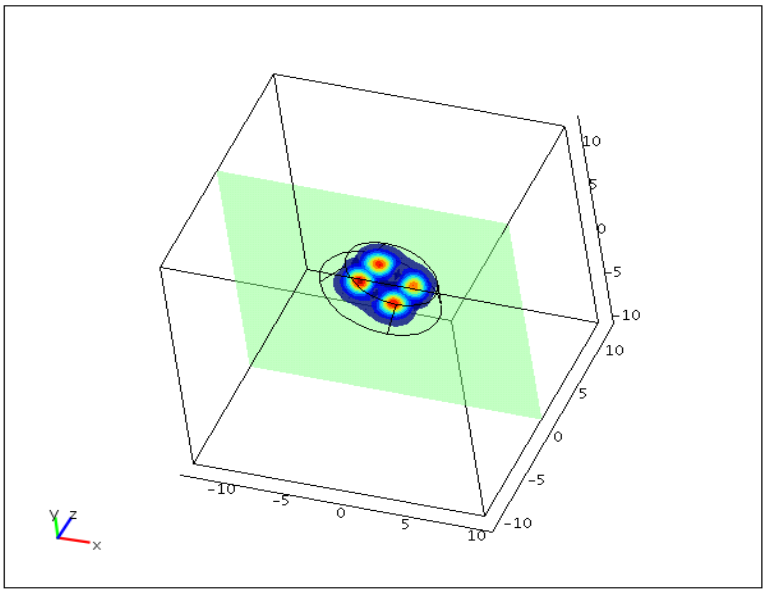

FIGURE 4. Quantum dot eigenstate that corresponds to the fifth eigenvalue

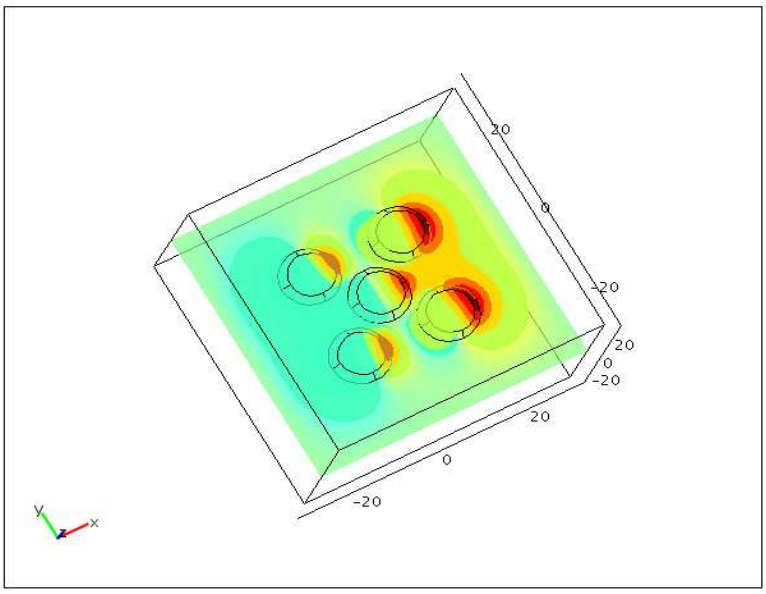

FIGURE 5. Five-dot quantum dot molecule: the x-component of displacement

7. **Concluding remarks.** Although there is a range of new effects that are fundamental to optoelectromechanical properties of LDSN, their influence is typically analyzed with simplified linear models based on the minimization of uncoupled, purely elastic energy functionals with respect to displacements. The applicability of such models is limited to the study of isolated idealized quantum dots, and both coupled and nonlinear effects need to be accounted for in the analysis of more realistic structures. Here, we have proposed generalizations of the existing models for bandstructure calculations in the context of strain effects and show how nonlinearities can be incorporated in the existing models. Examplifications have been given for hexagonal WZ semiconductor nanostructures.

REFERENCES

[1] Andreev, A.D. and O'Reilly, E.P., *Theory of the electronic structure of GaN/AlN hexagonal quantum dots*, Phys. Rev. B, **62** (2000), 15851–15870.

[2] Bir, G.L. and Pikus, G.E., "Symmetry and Strain-Induced Effects in Semiconductors", John Wiley and Sons, N.Y., 1974.

[3] Fonoberov, V.A., Balandin, A.A., *Electronic properties of strained wurtzite and zinc-blende $GaN/Al_xGa_{1-x}N$ quantum dots*, J. Appl. Phys., **94** (2003), 7178–7186.

[4] Jogai, B., Albrecht, J.D., and Pan, E., *Effect of electromechanical coupling on the strain in AlGaN/GaN HFETs*, J. Appl. Phys., **94** (2003), 3984–3989.

[5] Johnson, H.T. and Bose, R., *Nonoindentation effect on the optical properties of self-assembled quantum dots*, J. Mech. Phys. Solids, **51** (2003), 2085–2104.

[6] Lew Yan Voon, L.C., Melnik R., Lassen, B., and Willatzen, M., *Influence of aspect ratio on the lowest states of quantum rods*, Nano Letters, **4** (2004), 289–292.

[7] Markowich, P.A., Ringhofer, C.A., and Schmeiser, C., "Semiconductor Equations", Springer-Verlag, 1990.

[8] Melnik, R.V.N. and He, H., *Modelling nonlocal processes in semiconductor devices with exponential difference schemes*, J. of Eng. Mathematics, **38** (2000), 233–263.

[9] Melnik, R.V.N. and Willatzen, M., *Bandstructures of conical quantum dots with wetting layers*, Nanotechnology, **15** (2004), 1–8.

[10] Melnik, R.V.N. and Zotsenko, K.N., *Mixed electroelastic waves and CFL stability conditions in computational piezoelectricity*, Appl. Numerical Mathematics, **48** (2004), 41–62.

[11] Mireles, F. and Ulloa, S.E., *Strain and crystallographic orientation effects on the valence subbands of wirtzite quantum wells*, Phys. Rev. B, **62** (2000), 2562–2572.

[12] Oyafuso, F., Klimeck, G., von Allmen, P., Boykin, T., and Bowen, R.C., *Strain effects in large-scale atomistic quantum dot simulations*, Phys. Stat. Sol.(b), **239** (2003), 71–79.

[13] Schmidt, O.G. and Eberl, K., *Thin solid films roll up into nanotubes*, Nature, **410** (2001) 168.

[14] Willatzen, M., Melnik, R.V.N., C. Galeriu, Lew Yan Voon, L.C., *Quantum confinement phenomena in nanowire superlattice structures*, Mathematics and Computers in Simulation, **65** (2004), 385–397.

[15] Zaslavsky, A. et al, *Strain relaxation in silicon-germanium microstructures observed by resonant tunneling spectroscopy*, Appl. Phys. Let., **67** (1995), 3921.

Received September, 2004; revised May, 2005.

E-mail address: rmelnik@wlu.ca